Crystal structure of $Ca_2Zn_2(V_4O_{14})$ and $Pb_2Cd_2(V_3O_{10})(VO_4)$ double vanadates

V. D. Zhuravlev,[1,a)] A. P. Tyutyunnik,[1] A. Y. Chufarov,[1] N. I. Lobachevskaya,[1] and A. A. Velikodnyi[2]
[1]*Institute of Solid State Chemistry, Ural Branch, Russian Academy of Sciences, Pervomaiskaya ul. 91, Ekaterinburg 620990, Russia*
[2]*Faculty of Chemistry, Moscow State University, Moscow 119992, Russia*

(Received 11 July 2017; accepted 8 April 2018)

Polycrystalline samples of $Ca_2Zn_2(V_4O_{14})$ (I) and $Pb_2Cd_2(V_3O_{10})(VO_4)$ (II) were synthesized using the nitrate–citrate method (I) and conventional solid state reaction (II). The structural refinement based on X-ray powder diffraction data showed that the crystal structure of (I) is characterized by monoclinic symmetry with unit-cell parameters $a = 6.8044(1)$ Å, $b = 14.4876(3)$ Å, $c = 11.2367(2)$ Å, $\beta = 99.647(1)°$ [space group $P2_1/c$ (No. 14), $Z = 4$], and the crystal structure of (II) is triclinic with unit-cell parameters $a = 7.03813(6)$ Å, $b = 12.9085(1)$ Å, $c = 6.99961(5)$ Å, $\alpha = 90.7265(5)°$, $\beta = 96.3789(5)°$, $\gamma = 94.9530(6)°$, $V = 629.470(8)$ Å^3 [space group $P\bar{1}$ (No. 2), $Z = 2$]. © *2018 International Centre for Diffraction Data*. [doi:10.1017/S0885715618000441]

Key words: double vanadates, X-ray powder diffraction, crystal structure

I. INTRODUCTION

The pyrovanadates $M_2V_2O_7$, where M = Ca, Sr, Pb, Ba, Mg, Zn, Co, Ni, Cu, Mn, Cd, demonstrate promising magnetic (Bhatia *et al.*, 2010; Basiev *et al.*, 2011; Sanchez-Andujar *et al.*, 2011), optical (Cid-García *et al.*, 2012; Dalal *et al.*, 2015; Takahashi *et al.*, 2016), and electrical (Cowin *et al.*, 2011) properties. The physico-chemical properties and structures of divalent metal vanadates have been studied in depth. Double vanadates of nominal compositions $MM^IV_2O_7$ and $M_{1.5}M^I_{0.5}V_2O_7$, where M, M^I = Ca, Sr, Pb, Ba, Mg, Zn, Co, Ni, Cu, Mn, Cd, were synthesized mainly in the period between 1985 and 1999. At the same time, not only the unit-cell parameters were determined for a number of compounds, but also the crystal structures were described (Table I). A systematic study of the crystal structure of divalent metal vanadates has cast doubt on the correctness of isolation of the pyroanion $V_2O_7^{4-}$ in their chemical formula, since the data obtained showed a more complex anion structure (Zhuravlev *et al.*, 1982; Murashova *et al.*, 1989; Murashova *et al.*, 1991; Vogt and Muller-Buschbaum, 1991a). In addition to vanadates with anionic groups $V_2O_7^{4-}$, compounds containing anionic groups $V_4O_{14}^{8-}$ and $[(V_3O_{10})(VO_4)]^{8-}$ were also described. In Table I, a part of the formula of double vanadates is presented taking into account the data on the V–O distances in the vanadium–oxygen groups; the other part is presented in the form given in the original sources.

In this paper, the results of goal-oriented synthesis of double vanadates of calcium and zinc, lead, and cadmium (Table I) and their crystal structures are reported, and changes in the configuration and vanadium–oxygen polyhedra of related compounds are considered.

[a)]Author to whom correspondence should be addressed. Electronic mail: zhvd@ihim.uran.ru

II. EXPERIMENTAL

Samples of $Ca_2Zn_2(V_4O_{14})$ were synthesized using the citrate method. $Pb_2Cd_2(V_3O_{10})(VO_4)$ was obtained via solid-phase synthesis. Calcium–zinc and calcium–manganese vanadates were prepared by dissolving an equimolar amount of manganese (zinc) oxides and calcium carbonate of reactive purity in nitric acid. An equivalent amount of V_2O_5 was separately dissolved in citric acid in the ratio 1:4 during heating. After complete dissolution of the V_2O_5 sample, the vanadium solution acquired a blue colour, indicating the formation of vanadyl citrate,

$$V_2O_5 + 4C_6H_8O_7 = 2(VO)(C_6H_7O_7)_2 + H_2O + O_2\uparrow$$

The formation of nitrate–citrate complexes followed the coacervation of vanadyl citrate solutions and nitrates of calcium, manganese, and zinc, preventing salting out and leading, under heating, to the formation of xerogels of variable composition. Evaporation was carried out at about 100 °C until a viscous mass was formed. After the formation of the xerogel, the temperature was raised to 250–300 °C, initiating a redox process in the reaction mass. The reaction proceeded without release of nitrogen oxides because of the excess of citric acid reducing agent. The resulting powder was brownish-yellow because of the presence of unburned carbon particles. The precursor was ground in an agate mortar and annealed at 500 and 650 °C, whereupon the product acquired a white colour. According to XRPD, it became single phase after annealing at ~650 °C.

$Pb_2Cd_2(V_3O_{10})(VO_4)$ was synthesized using cadmium carbonate, lead oxide, and vanadium (V) oxide. The initial components were mixed and subjected to multistage annealing in the temperature range from 450 to 600 °C. The annealing time at the final stage of synthesis was 30 h.

The X-ray powder diffraction (XRPD) patterns were collected at room temperature on a STADI P (Stoe)

TABLE I. Crystallographic characteristics of double vanadates of divalent metals.

Compound	*a* (Å)	*b* (Å)	*c* (Å)	*β* (°)	*Z*	Sp.gr.	References
I							
$Sr_2Mg_2(V_4O_{14})$	6.829 (2)	14.857 (4)	11.309 (4)	98.78 (2)	4	$P2_1/c$	Velikodnyi *et al.* (1985)
$SrCoV_2O_7$	6.8360 (20)	14.822 (2)	11.2710 (10)	99.430 (20)	8	$P2_1/c$	PDF 00-044-455
$SrMnV_2O_7$	6.876 (1)	15.031 (3)	11.591 (2)	96.96 (2)	8	$P2_1/c$	Zhuravlev *et al.* (1993)
$Pb_2Zn_2(V_4O_{14})$	6.911 (2)	14.853 (2)	11.338 (2)	99.51 (1)	4	$P2_1/c$	Murashova *et al.* (1991)
Pb_2Mg_2 $(V_3O_{10})(VO_4)$	6.854 (1)	15.007 (5)	11.490 (2)	97.84 (2)	4	$P2_1/c$	Murashova *et al.* (1991)
$PbCoV_2O_7$	6.8657 (7)	14.8610 (20)	11.3300 (20)	99.590 (10)	8	$P2_1/c$	PDF 00-051-0134
$Pb_2Mn_2(V_3O_{10})(VO_4)$	6.9255 (6)	15.0841 (10)	11.6710 (10)	97.006 (8)	4	$P2_1/c$	PDF 00-051-0418
Ca_2Mg_2 (V_4O_{14})	6.756 (2)	14.495 (3)	11.253 (2)	99.12 (2)	8	$P2_1/c$	Murashova *et al.* (1993)
Ca_2Co_2 (V_4O_{14})	6.769 (1)	14.472 (2)	11.225 (2)	99.52 (1)	4	$P2_1/c$	Murashova *et al.* (1993)
$Ca_2Zn_2(V_4O_{14})$	6.8044 (1)	14.4876 (3)	11.2367 (2)	99.647 (1)	4	$P2_1/c$	*
II							
$SrCuV_2O_7$	14.496 (2)	5.469 (1)	7.425 (1)		4	*Pnma*	Vogt, and Muller-Buschbaum (1991b)
$BaCuV_2O_7$	15.0511 (69)	5.5136 (24)	7.5134 (17)		4	*Pnma*	Vogt, and Muller-Buschbaum (1991a)
$BaCaV_2O_7$	15.508 (3)	5.814 (1)	7.343 (2)		4	*Pnma*	Murashova *et al.* (1989)
α-$BaZnV_2O_7$	15.048 (3)	5.5700 (10)	7.55580 (20)		4	*Pnma*	Murashova *et al.* (1989)
$BaCdV_2O_7$	15.400 (2)	5.712 (1)	7.412 (1)		4	*Pnma*	Murashova *et al.* (1989)
$BaMgV_2O_7$	15.062 (2)	5.5799 (1)	7.578 (1)		4	*Pnma*	PDF 00-046-0758
III							
β-$BaZnV_2O_7$	5.573 (1)	15.175 (1)	7.429 (1)	96.45 (1)	4	$P2_1/n$	Murashova *et al.* (1989)
$BaMnV_2O_7$	5.623 (1)	15.287 (3)	7.401 (2)	95.55 (2)	4	$P2_1/n$	Zhuravlev *et al.* (1993)
$SrZnV_2O_7$	7.425 (2)	6.697 (2)	11.977 (5)	95.98 (5)	4	$P2_1/n$	Velikodnyi *et al.* (1989)
IV							
$Sr_3Mn(V_2O_7)_2$	6.997 (1)		25.443 (8)		4	$P4_12_12$	Zhuravlev *et al.* (1993)
$Sr_3Ca(V_2O_7)_2$	7.012		25.4500		4	$P4_1$	Zhuravlev *et al.* (1990)
$Sr_3Cd(V_2O_7)_2$	7.057 (1)		25.566 (2)		4	$P4_12_12$	Velikodnyi *et al.* (1993a)
V							
$Pb_2Cd_2(V_3O_{10})(VO_4)$[a]	6.99961 (5)	7.03813 (6)	12.9085 (1)	94.9530 (5) 90.7265 (5) 96.3789 (5)	2	$P\bar{1}$	[b]
$Ba_3PbV_4O_{14}$[a]	7.2932 (15)	7.2997 (15)	13.379 (3)	99.68 (3) 93.68 (3) 91.49 (3)	2	$P\bar{1}$	Sivakumar *et al.* (2007)
VI							
$CaCuV_2O_7$	10.010 (37)	8.8454 (51)	10.1899 (19)	91.032 (17)	8	*P2/c*	Vogt and Muller-Buschbaum (1991b)

[a]The reduced cells are shown.
[b]Data obtained in this study.

TABLE II. Crystal data and structure refinement for $Ca_2Zn_2(V_4O_{14})$ and $Pb_2Cd_2(V_3O_{10})(VO_4)$.

Structure formula	$Ca_2Zn_2(V_3O_{10})(VO_4)$	$Pb_2Cd_2(V_3O_{10})(VO_4)$
Formula weight, Mr, g/mol	638.69	1066.974
Temperature, K	298 (2)	298 (2)
Crystal system, space group	Monoclinic, $P2_1/c$ (No. 14)	Triclinic, $P\bar{1}$ (No. 2)
Unit-cell parameters		
a, Å	6.8093 (2)	7.03813 (6)
b, Å	14.5094 (3)	12.9085 (1)
c, Å	11.2568 (3)	6.99961 (5)
α, ∘	90	90.7265 (5)
β, ∘	99.471 (12)	96.3789 (5)
γ, ∘	90	94.9530 (5)
V, Å^3	1092.8 (3)	629.470 (8)
Formula unit, *Z*	4	2
Calculated density, g/cm^3	3.881	5.629
Measured density, g/cm^3	3.865 (5)	
wR_p, %	2.04	2.17
R_p, %	1.56	1.58
χ^2	4.02	1.975
$R(F^2)$, %	2.50	2.57

https://doi.org/10.1017/S0885715618000441 Published online by Cambridge University Press

TABLE III. Atomic coordinates and isotropic displacement parameters ($U_{iso} \times 100$, Å^2) for $Ca_2Zn_2(V_4O_{14})$ and $Pb_2Cd_2(V_3O_{10})(VO_4)$.

Atom	*X*	*Y*	*z*	$U_{iso} \times 100$
$Ca_2Zn_2(V_4O_{14})$				
Zn(1)	−0.0089 (9)	0.25215 (29)	0.24720 (43)	4.01 (10)
Zn(2)	0.3428 (6)	0.17318 (28)	0.42497 (35)	4.01 (10)
Ca(1)	0.6571 (9)	0.1315 (5)	0.0201 (5)	4.9 (2)
Ca(2)	0.9461 (8)	0.0053 (5)	0.7552 (5)	4.9 (2)
V(1)	0.4870 (9)	0.2099 (4)	0.7063 (5)	3.27 (7)
V(2)	0.4297 (8)	0.0171 (4)	0.6888 (5)	3.27 (7)
V(3)	0.1397 (9)	−0.1347 (4)	0.5203 (6)	3.27 (7)
V(4)	0.1558 (9)	0.3765 (5)	0.5137 (5)	3.27 (7)
O(1)	0.5681 (20)	0.1095 (12)	0.7928 (12)	2.27 (13)
O(2)	0.2934 (28)	0.2615 (10)	0.7657 (15)	2.27 (13)
O(3)	0.3293 (26)	0.2937 (11)	0.5297 (16)	2.27 (13)
O(4)	0.6764 (28)	0.2754 (11)	0.7040 (14)	2.27 (13)
O(5)	0.3925 (21)	0.1137 (12)	0.5951 (13)	2.27 (13)
O(6)	0.6135 (22)	−0.0458 (11)	0.6799 (14)	2.27 (13)
O(7)	0.2467 (22)	−0.0209 (12)	0.5481 (13)	2.27 (13)
O(8)	0.2945 (25)	−0.0097 (12)	0.7964 (14)	2.27 (13)
O(9)	−0.0348 (24)	−0.1596 (11)	0.6241 (15)	2.27 (13)
O(10)	0.0433 (22)	−0.1270 (12)	0.3721 (16)	2.27 (13)
O(11)	0.3384 (25)	−0.2128 (10)	0.5510 (15)	2.27 (13)
O(12)	0.0000 (26)	0.3713 (13)	0.3686 (14)	2.27 (13)
O(13)	−0.0041 (25)	0.3572 (12)	0.6169 (15)	2.27 (13)
O(14)	0.2589 (24)	0.4809 (13)	0.5298 (14)	2.27 (13)
$Pb_2Cd_2(V_3O_{10})(VO_4)$				
Pb(1)	0.38527 (19)	0.15779 (10)	0.39246 (19)	2.78 (13)
Pb(2)	0.68426 (20)	0.40938 (11)	0.14207 (19)	3.42 (13)
Cd(1)	0.13147 (31)	0.38557 (17)	0.49405 (30)	1.15 (14)
Cd(2)	0.29542 (31)	0.85660 (16)	0.12174 (31)	2.09 (14)
V(1)	0.8514 (8)	0.1271 (5)	0.3866 (8)	3.33 (23)
V(2)	0.8023 (8)	0.9146 (4)	0.1311 (8)	2.70 (23)
V(3)	0.1452 (7)	0.3175 (4)	0.9992 (8)	3.54 (21)
V(4)	0.6417 (7)	0.3891 (4)	0.6537 (8)	2.30 (22)
O(1)	0.9293 (21)	0.0097 (15)	0.2764 (22)	2.85 (17)[a]
O(2)	0.9516 (22)	0.8143 (13)	0.0749 (21)	2.85 (17)[a]
O(3)	0.2810 (20)	0.9044 (11)	0.4338 (24)	2.85 (17)[a]
O(4)	0.7112 (21)	0.1813 (11)	0.2063 (22)	2.85 (17)[a]
O(5)	0.0568 (22)	0.2043 (11)	0.4654 (20)	2.85 (17)[a]
O(6)	0.6232 (22)	0.8650 (12)	0.2328 (23)	2.85 (17)[a]
O(7)	0.7200 (21)	0.9781 (12)	0.9449 (24)	2.85 (17)[a]
O(8)	0.1697 (21)	0.4023 (12)	0.8182 (22)	2.85 (17)[a]
O(9)	0.3510 (21)	0.2843 (11)	0.1006 (21)	2.85 (17)[a]
O(10)	0.0387 (22)	0.3667 (12)	0.1799 (24)	2.85 (17)[a]
O(11)	0.7462 (23)	0.3052 (12)	0.8085 (21)	2.85 (17)[a]
O(12)	0.4360 (25)	0.3357 (12)	0.5068 (23)	2.85 (17)[a]
O(13)	0.8135 (20)	0.4379 (12)	0.4978 (22)	2.85 (17)[a]
O(14)	0.5817 (21)	0.4849 (11)	0.7821 (21)	2.85 (17)[a]

[a]Atomic displacement parameters of all oxygen atoms were constrained as single variable.

diffractometer with transmission geometry, using Cu$K\alpha_1$ radiation and a linear mini-PSD detector in a 2θ range of 5–120° with a step of 0.02°. To obtain high-quality diffraction data, following the recommendations given by Stoe, very thin layers of powdered high absorbing materials were fixed on acetate foils by Elmers White Glue. The thickness of the layer was adjusted to get the transmission factor, I_0/I, equal to approximately 2–3, where I_0 is the flux of the primary beam, and I is the flux passing through the specimen. Polycrystalline silicon [$a = 5.43075(5)$ Å] was used as an external standard. Possible impurity phases were checked by comparing their XRPD patterns with those in the PDF2 database (ICDD, 2016). The only impurity found was 1.5 mass% of $Cd_2V_2O_7$ in $Pb_2Cd_2(V_3O_{10})(VO_4)$. The XRPD pattern of $Ca_2Zn_2(V_4O_{14})$ was indexed using the TREOR program (Werner *et al.*, 1985) and compared with an analogous monoclinic unit cell of $CaCoV_2O_7$ (Murashova *et al.*, 1993). The crystal structure refinement of the new compounds was carried out employing Rietveld analysis (Rietveld, 1969) with the GSAS program suite using the XRPD data (Toby, 2001; Larson and Von Dreele, 2004). The peak profiles were fitted with a pseudo-Voigt function, $I(2\theta) = x \times L(2\theta) + (1-x) \times G(2\theta)$ (where L and G are the Lorentzian and Gaussian parts, respectively). The angular dependence of the peak width was described by the relation $(\text{FWHM})^2 = Utg^2\theta + Vtg\theta + W$, where FWHM is the full line width at half maximum. The background level was described by a combination of 15-order Chebyshev polynomials. Since the background of XRPD pattern of $Pb_2Cd_2(V_3O_{10})(VO_4)$ was difficult to fit, it was removed before the refinement. The absorption correction function for a flat plate sample in transmission geometry was applied. Since both models being refined have a large number of atomic positions, and correlations

https://doi.org/10.1017/S0885715618000441 Published online by Cambridge University Press

TABLE IV. Selected interatomic distances d (Å) and angles (°) for $Ca_2Zn_2(V_4O_1)$ and $Pb_2Cd_2(V_3O_{10})(VO_4)$.

(a) $Ca_2Zn_2(V_4O_{14})$

Interatomic distances		Interatomic distances		Interatomic distances		Interatomic distances	
Zn(1)–O(2)	2.042 (18)	Zn(2)–O(2)	2.002 (16)	Ca(1)–O(1)	2.545 (13)	Ca(2)–O(6)	2.396 (15)
Zn(1)–O(4)	2.152 (19)	Zn(2)–O(3)	2.116 (16)	Ca(1)–O(3)	2.498 (17)	Ca(2)–O(8)	2.348 (17)
Zn(1)–O(9)	1.958 (15)	Zn(2)–O(5)	2.072 (15)	Ca(1)–O(4)	2.452 (16)	Ca(2)–O(9)	2.820 (17)
Zn(1)–O(10)	2.194 (20)	Zn(2)–O(6)	2.237 (17)	Ca(1)–O(8)	2.692 (16)	Ca(2)–O(10)	2.280 (18)
Zn(1)–O(12)	2.195 (18)	Zn(2)–O(9)	2.085 (16)	Ca(1)–O(11)	2.395 (17)	Ca(2)–O(12)	2.191 (19)
Zn(1)–O(13)	2.161 (16)	Zn(2)–O(11)	2.216 (17)	Ca(1)–O(13)	2.384 (18)	Ca(2)–O(13)	2.575 (18)
				Ca(1)–O(14)	2.347 (19)		
Zn–O	**2.117**	**Zn–O**	**2.121**	**Ca–O**	**2.473**	**Ca–O**	**2.435**
Expected[a]	*2.100*	*Expected*[a]	*2.100*	*Expected*[a]	*2.420*	*Expected*[a]	*2.420*
V(1)–O(1)	1.785 (15)	V(2)–O(1)	1.918 (15)	V(3)–O(7)	1.809 (17)	V(4)–O(3)	1.671 (16)
V(1)–O(2)	1.742 (16)	V(2)–O(5)	1.745 (16)	V(3)–O(9)	1.834 (16)	V(4)–O(12)	1.792 (15)
V(1)–O(3)	2.418 (18)	V(2)–O(6)	1.563 (15)	V(3)–O(10)	1.688 (14)	V(4)–O(13)	1.740 (14)
V(1)–O(4)	1.604 (16)	V(2)–O(7)	1.921 (15)	V(3)–O(11)	1.752 (16)	V(4)–O(14)	1.665 (17)
V(1)–O(5)	1.909 (16)	V(2)–O(8)	1.682 (16)				
V–O	**1.892**	**V–O**	**1.766**	**V–O**	**1.771**	**V–O**	**1.717**
Expected[a]	*1.820*	*Expected*[a]	*1.820*	*Expected*[a]	*1.715*	*Expected*[a]	*1.715*
Angles		Angles		Angles			
O(1)V(1)O(2)	109.0 (8)	O(1)V(2)O(5)	79.3 (6)	O(7)V(3)O(9)	110.7 (8)	O(3)V(4)O(12)	111.6 (10)
O(1)V(1)O(3)	155.6 (7)	O(1)V(2)O(6)	97.4 (8)	O(7)V(3)O(10)	100.9 (9)	O(3)V(4)O(13)	108.8 (9)
O(1)V(1)O(4)	108.3 (8)	O(1)V(2)O(7)	152.3 (8)	O(7)V(3)O(11)	106.2 (7)	O(3)V(4)O(14)	111.3 (8)
O(1)V(1)O(5)	78.5 (7)	O(1)V(2)O(8)	89.7 (8)	O(9)V(3)O(10)	117.0 (8)	O(12)V(4)O(13)	105.0 (7)
O(2)V(1)O(3)	80.7 (7)	O(5)V(2)O(6)	117.7 (8)	O(9)V(3)O(11)	108.0 (8)	O(12)V(4)O(14)	108.1 (9)
O(2)V(1)O(4)	114.4 (8)	O(5)V(2)O(7)	74.0 (7)	O(10)V(3)O(11)	113.3 (8)	O(13)V(4)O(14)	111.9 (9)
O(2)V(1)O(5)	111.8 (7)	O(5)V(2)O(8)	125.2 (8)				
O(3)V(1)O(4)	86.4 (7)	O(6)V(2)O(7)	101.3 (7)				
O(3)V(1)O(5)	77.0 (6)	O(6)V(2)O(8)	116.8 (9)				
O(4)V(1)O(5)	127.2 (8)	O(7)V(2)O(8)	99.7 (8)				

(b) $Pb_2Cd_2(V_3O_{10})(VO_4)$

Interatomic distances		Interatomic distances		Interatomic distances		Interatomic distances	
Pb(1)–O(3)	2.712 (14)	Pb(2)–O(4)	3.003 (15)	Cd(1)–O(5)	2.355 (15)	Cd(2)–O(2)	2.419 (15)
Pb(1)–O(4)	2.758 (13)	Pb(2)–O(8)	2.555 (16)	Cd(1)–O(8)	2.261 (15)	Cd(2)–O(3)	2.278 (16)
Pb(1)–O(5)	2.542 (14)	Pb(2)–O(9)	2.715 (15)	Cd(1)–O(10)	2.227 (17)	Cd(2)–O(4)	2.336 (14)
Pb(1)–O(6)	2.650 (15)	Pb(2)–O(10)	2.587 (15)	Cd(1)–O(12)	2.284 (15)	Cd(2)–O(6)	2.344 (15)
Pb(1)–O(7)	2.912 (15)	Pb(2)–O(11)	2.775 (14)	Cd(1)–O(13)	2.396 (14)	Cd(2)–O(7)	2.200 (15)
Pb(1)–O(9)	2.635 (14)	Pb(2)–O(13)	2.565 (15)	Cd(1)–O(13)	2.277 (15)	Cd(2)–O(11)	2.153 (15)
Pb(1)–O(12)	2.406 (15)	Pb(2)–O(14)	2.757 (14)				
			Pb(2)–O(14)	2.508(15)			
Pb–O	**2.659**	**Pb–O**	**2.683**	**Cd–O**	**2.3**	**Cd–O**	**2.288**
Expected[a]	*2.59*	*Expected*[a]	*2.65*	*Expected*[a]	*2.31*	*Expected*[a]	*2.31*
V(1)–O(1)	1.844 (16)	V(2)–O(1)	1.707 (16)	V(3)–O(2)	1.824 (15)	V(4)–O(11)	1.697 (15)
V(1)–O(3)	1.680 (14)	V(2)–O(2)	1.803 (15)	V(3)–O(8)	1.698 (14)	V(4)–O(12)	1.763 (18)
V(1)–O(4)	1.709 (15)	V(2)–O(6)	1.606 (14)	V(3)–O(9)	1.634 (13)	V(4)–O(13)	1.796 (15)
V(1)–O(5)	1.717 (15)	V(2)–O(7)	1.627 (16)	V(3)–O(10)	1.685 (15)	V(4)–O(14)	1.632 (14)
V–O	**1.738**	**V–O**	**1.686**	**V–O**	**1.71**	**V–O**	**1.722**
Expected[a]	*1.715*	*Expected*[a]	*1.715*	*Expected*[a]	*1.715*	*Expected*[a]	*1.715*
Angles		Angles		Angles			
O(1)V(1)O(3)	110.9 (7)	O(1)V(2)O(2)	111.3 (8)	O(2)V(3)O(8)	115.6 (8)	O(11)V(4)O(12)	115.1 (8)
O(1)V(1)O(4)	105.0 (7)	O(1)V(2)O(6)	110.0 (8)	O(2)V(3)O(9)	95.6 (8)	O(11)V(4)O(13)	108.8 (7)
O(1)V(1)O(5)	106.3 (8)	O(1)V(2)O(7)	103.2 (8)	O(2)V(3)O(10)	113.3 (8)	O(11)V(4)O(14)	107.3 (8)
O(3)V(1)O(4)	109.1 (8)	O(2)V(2)O(6)	109.9 (7)	O(8)V(3)O(9)	112.8 (8)	O(12)V(4)O(13)	107.5 (7)
O(3)V(1)O(5)	112.1 (8)	O(2)V(2)O(7)	113.8 (8)	O(8)V(3)O(10)	112.9 (8)	O(12)V(4)O(14)	108.6 (7)
O(4)V(1)O(5)	113.1 (7)	O(6)V(2)O(7)	108.3 (8)	O(9)V(3)O(10)	104.9 (8)	O(13)V(4)O(14)	109.5 (8)
V(1)O(1)V(2)	130.6 (9)	V(2)O(2)V(3)	122.9 (9)				

The average values are indicated by boldface type.

[a]The sum of the crystal radii according to [Shannon R.D. Acta Crystallogr. A 32 (1976) 751]: Pb^{+2} VII – 1.37 Å, Pb^{+2} VIII – 1.43 Å, Cd^{+2} VI – 1.09 Å, V^{+5} IV – 0.495 Å, O^{-2} III – 1.22 Å.

between a large number of variables are probable, the atomic displacement parameters of all oxygen atoms were constrained as single variable. The crystallographic data, atomic coordinates, atomic displacement parameters, and selected interatomic distances are given in Tables II–IV. Experimental, calculated, and difference XRPD patterns are shown in Figure 1.

Density measurements were carried out on an AccuPyc II 1340 Gas Displacement Pycnometry System (Micromeritics Instrument Corporation, Norcross, Georgia, USA) with a sample chamber of 1 cm^3. About 50–60% of the chamber volume was filled by the powder sample; 15 measurements were performed on the sample.

https://doi.org/10.1017/S0885715618000441 Published online by Cambridge University Press

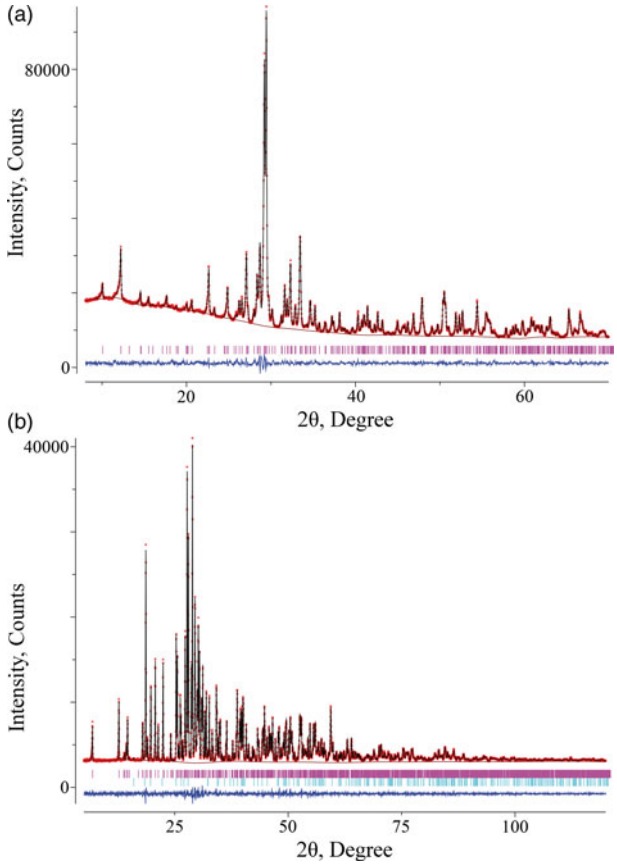

Figure 1. (Color online) Experimental (crosses), calculated (solid line), and difference (bottom line) XRPD patterns of (a) $Ca_2Zn_2(V_4O_{14})$ and (b) $Pb_2Cd_2(V_3O_{10})(VO_4)$. The tick marks correspond to the Bragg reflections.

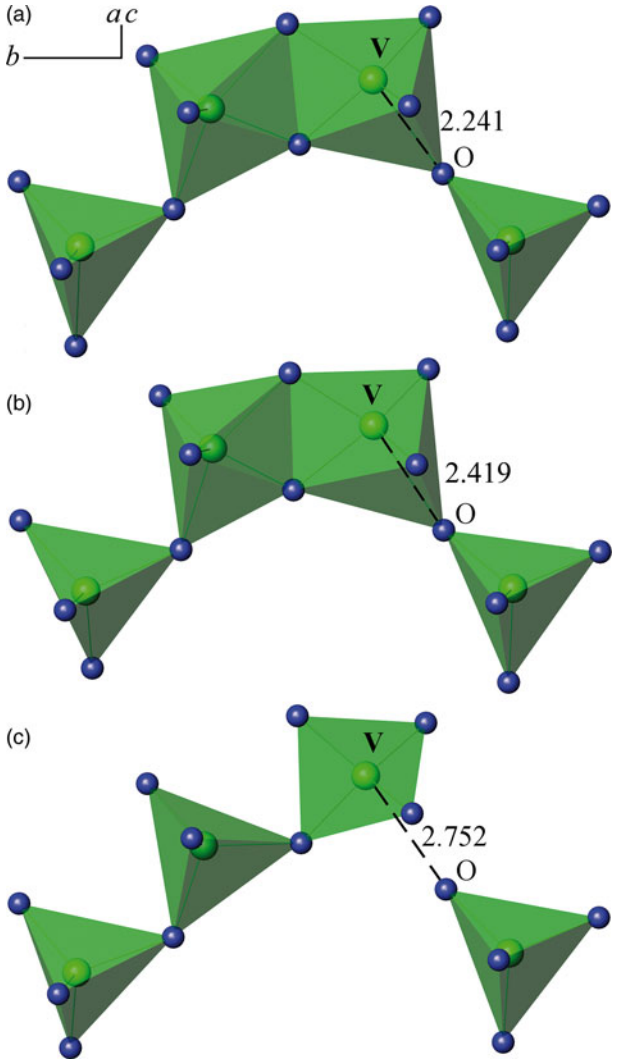

Figure 2. (Color online) The connection of anionic groups in vanadates $Pb_2Zn_2(V_4O_{14})$ (a), $Ca_2Zn_2(V_4O_{14})$ (b), $Pb_2Mg_2(V_3O_{10})(VO_4)$ (d).

III. DISCUSSION

The XRPD pattern of $Ca_2Zn_2(V_4O_{14})$ was indexed in the monoclinic system with unit-cell parameters $a = 6.8044(1)$ Å, $b = 14.4876(3)$ Å, $c = 11.2367(2)$ Å, $\beta = 99.647(1)°$ [space group $P2_1/c$ (14), $Z = 4$]. The most representative double vanadates belong to group I consisting of 10 compounds having an isotype structure that crystallizes in monoclinic system with space group $P2_1/c$. Their nominal anions $V_2O_7^{4-}$ either condense into $V_4O_{14}^{8-}$ tetramers when the oxygen coordination of the vanadium atoms increases to five [Figures 2(a) and 2(b)], or they form a pair of $V_3O_{10}^{5-}$ trimer and orthovanadate ion VO_4^{3-} [Figure 2(c)]. This division into the isotype series is rather arbitrary since the increased V–O distance varies from 2.24 Å in $Pb_2Zn_2(V_4O_{14})$ to 2.75 Å in the trimer–orthovanadate–ion chain in $Pb_2Mg_2(V_3O_{10})(VO_4)$. This compound is represented as $Ca_2Zn_2(V_3O_{10})(VO_4)$ (Babaryk *et al.*, 2015). Crystal structure of $Ca_2Zn_2(V_4O_{14})$ consists of layers containing $V_4O_{14}^{8-}$ tetramers alternating along $(10\bar{2})$ direction with the layers of edge-sharing zinc–oxygen octahedra, Ca(1) and Ca(2) atoms fill empty sites in the latter with coordination numbers 7 and 6, respectively. $V_4O_{14}^{8-}$ group consists of two highly distorted edge-sharing vanadium–oxygen polyhedra with CN = 5, which share corners with two terminal vanadium–oxygen tetrahedra [Figures 2(b)], wherein V(1)–O(3) distance, 2.418 Å, is much longer than others. This confirms the separation of the orthovanadate ion VO_4^{3-} from $V_3O_{10}^{5-}$ trimer, proposed by Babaryk *et al.* (2015). At the same time, the average metal–oxygen distances are in good agreement with the sums of the crystal radii according to Shannon (1976).

The XRPD pattern of the obtained $Pb_2Cd_2(V_3O_{10})(VO_4)$ was found to be in good agreement with the data presented by Shpanchenko and Antipov in PDF2 (Entry 00-058-0617) for $PbCdV_2O_7$ and it was indexed with triclinic unit-cell parameters $a = 7.03813(6)$ Å, $b = 12.9085(1)$ Å, $c = 6.99961(5)$ Å, $\alpha = 90.7265(5)°$, $\beta = 96.3789(5)°$, $\gamma = 94.9530(6)°$, $V = 629.470(8)$ Å^3 (space group $P\bar{1}$, No. 2, $Z = 2$), the reduced cell is $a = 6.99961(5)$ Å, $b = 7.03813(6)$ Å, $c = 12.9085(1)$ Å, $\alpha = 94.9530(6)°$, $\beta = 90.7265(5)°$, $\gamma = 96.3789(5)°$. Such unit-cell parameters may be indicative of a similarity of the structure to the *B*-type rare-earth disilicates $RE_2Si_2O_7$ (Felsche, 1970). The crystal structure of $PbCdV_2O_7$ has been solved space group $P\bar{1}$ using the EXPO2013 program suite (Altomare *et al.*, 2013) assuming two formula units per unit cell. The resulting model shown in Figure 3, similarly to the structure of $Ca_2Zn_2(V_4O_{14})$, consists of layers containing $V_4O_{14}^{8-}$ groups alternating along the $(1\bar{1}\ 1)$ direction with the layers of two edge-sharing Cd(1)–oxygen octahedra and separate $Cd(2)O_6$ octahedra, Pb(1) and Pb(2) atoms fill empty sites in the latter with coordination numbers 7 and 8, respectively, forming a finite chain of four edge-sharing

https://doi.org/10.1017/S0885715618000441 Published online by Cambridge University Press

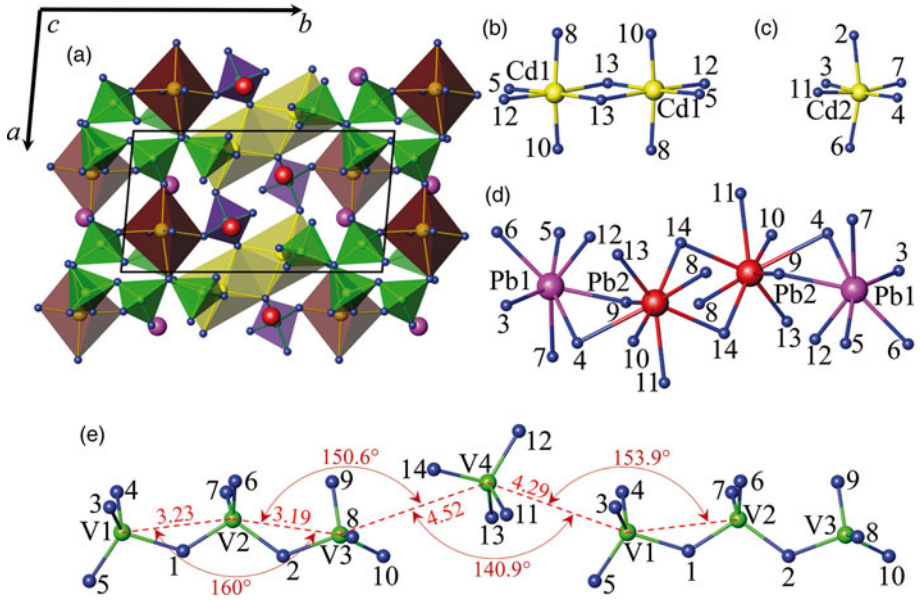

Figure 3. (Color online) Schematic drawing: (a) polyhedral view of the $Pb_2Cd_2(V_3O_{10})(VO_4)$ structure, (b) and (c) stick and ball representation of the edge-sharing and isolated $Cd(1)O_6$ and $Cd(2)O_6$ octahedra, respectively, (d) isolated unit built of four edge-sharing $Pb(1)O_7$ and $Pb(2)O_8$ polyhedra, (e) broken chain consisting of alternating single orthovanadate $(VO_4)^{3-}$ and linear trivanadate $(V_3O_{10})^{5-}$ group. Green and purple tetrahedra indicate tri- and orthovanadates, yellow and brown colour indicate edge-sharing and single cadmium–oxygen octahedra. Blue, purple, red, yellow, and green spheres indicate oxygen, Pb(1), Pb(2), cadmium, and vanadium sites, respectively.

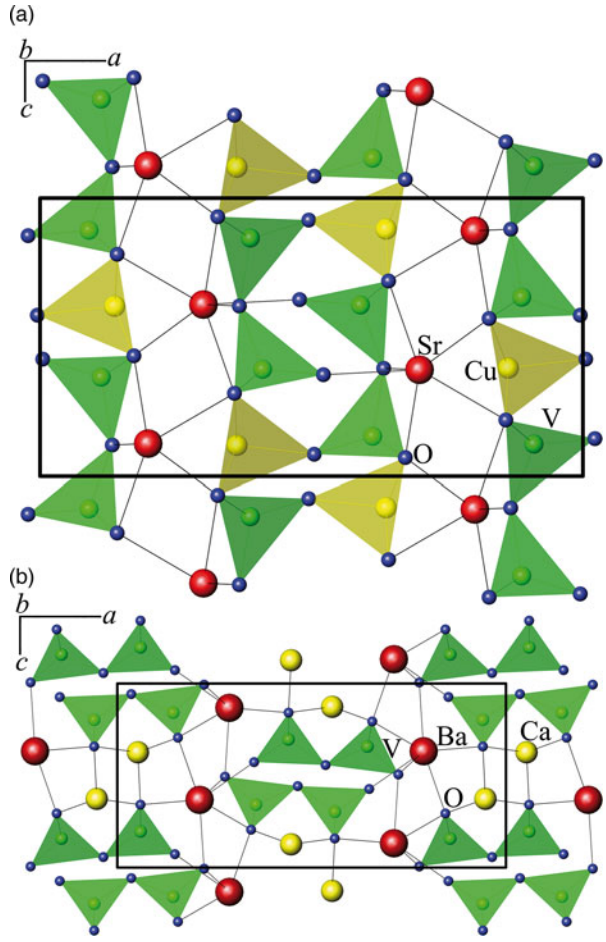

Figure 4. (Color online) The projection along the ***b***-axis of the structure of (a) $SrCuV_2O_7$ (Velikodnyi and Murashova, 1992) and (b) $BaCaV_2O_7$ (Murashova *et al.*, 1989).

polyhedra. In $Pb_2Cd_2(V_3O_{10})(VO_4)$, $V_4O_{14}{}^{8-}$ group contains broken chains unusual for the vanadates consisting of single orthovanadate $[V(4)O_4]^{3-}$ and linear trivanadate $(V_3O_{10})^{5-}$, formed of three sufficiently regular corner-sharing tetrahedra, alternating along (011) [Figure 3(e)]. The average metal–oxygen distances are in good agreement with the sums of the crystal radii according to Shannon (Shannon, 1976). Such a combination of triple tetrahedra $(Si_3O_{10})^{8-}$ and single tetrahedra $(SiO_4)^{4-}$ groups has been reported for $Ho_2Si_2O_7$ (Felsche, 1972). Owing to the decrease in the unit-cell symmetry in Table I, the compound constitutes a separate group V. The compound $Ba_3PbV_4O_{14}$ (Sivakumar *et al.*, 2007) is also referred to this group, although this contradicts the study of phase equilibria in the $Ba_2V_2O_7$–$Pb_2V_2O_7$ system. Primary solid solutions based on barium pyrovanadate were found to contain 0–30 mol% $Pb_2V_2O_7$ (Zhuravlev and Velikodnyi, 1997).

The authors also investigated the possibility of formation of $Pb_{1.5}Cd_{0.5}(V_3O_{10})(VO_4)$ and $Pb_{0.5}Cd_{1.5}(V_3O_{10})(VO_4)$ compounds. It was found that both compositions contain two phases: $Pb_2Cd_2(V_3O_{10})(VO_4)$ and $Pb_2V_2O_7$ or $Pb_2Cd_2(V_3O_{10})(VO_4)$ and $Cd_2V_2O_7$.

In group II of Table I, there are six compounds that crystallize in the orthorhombic system with space group *Pnma*. However, according to the $V_2O_7{}^{4-}$ anion packing, four compounds isotypic with $SrCuV_2O_7$ (Vogt and Muller-Buschbaum, 1991b) can be identified, with $V_2O_7{}^{4-}$ dimers elongated along the ***a***-axis [Figure 4(a)], while in the other two double pyrovanadates, $BaCaV_2O_7$ and α-$BaZnV_2O_7$ (high-temperature modification), $V_2O_7{}^{4-}$ dimers are elongated along the ***c***-axis [Figure 4(b)] (Murashova *et al.*, 1989).

Three double vanadates in group III form compounds with monoclinic symmetry and space group $P2_1/n$. Figure 5 displays a typical structure of β-$BaZnV_2O_7$ (Murashova

https://doi.org/10.1017/S0885715618000441 Published online by Cambridge University Press

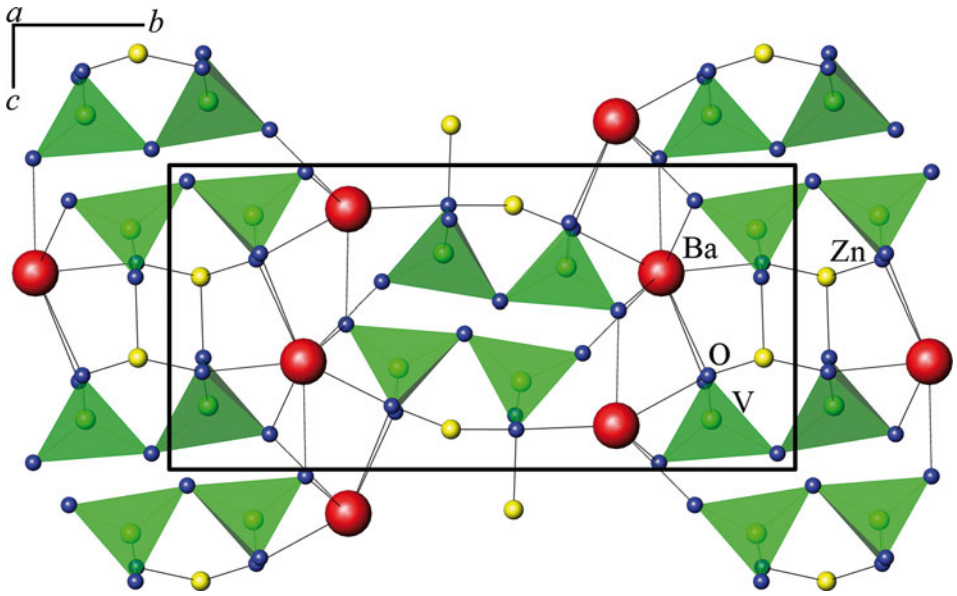

Figure 5. (Color online) Crystal structure of β-$BaZnV_2O_7$ (Murashova *et al.*, 1989).

et al., 1989). In group III, the vanadate $SrZnV_2O_7$ (Velikodnyi *et al.*, 1989) is also included, assuming the possibility of a different setting when indicating the parameters, namely: $a' = c/2 = 5.9885$ Å, $b' = 2a = 14.85$ Å, $c' = b = 6.697$ Å.

The double vanadate $CaCuV_2O_7$ (Figure 6) stands apart, since its $V_2O_7^{4-}$ chains are directed along the ***ac*** vector (Vogt and Muller-Buschbaum, 1991a; b)

The compound $CaCdV_2O_7$ (Krasnenko *et al.*, 1990) is not shown in Table I because, in the authors" opinion, it comprises a part of the solid solution based on cadmium pyrovanadates. The limiting composition of the homogeneity region is restricted by the sample $Ca_{1.22}Cd_{0.78}V_2O_7$ (Murashova *et al.*, 1994).

In the binary systems of vanadates of bivalent metals $Sr_2V_2O_7$–$M^I{}_2V_2O_7$ (M^I = Mn, Ca, Cd) (Velikodnyi and Murashova, 1992; Zhuravlev *et al.*, 1993; Zhuravlev *et al.*, 1994), compounds with cation ratio Sr:M^I = 3:1, crystallizing in tetragonal symmetry with space group $P4_12_12$ in Sr_3Mn

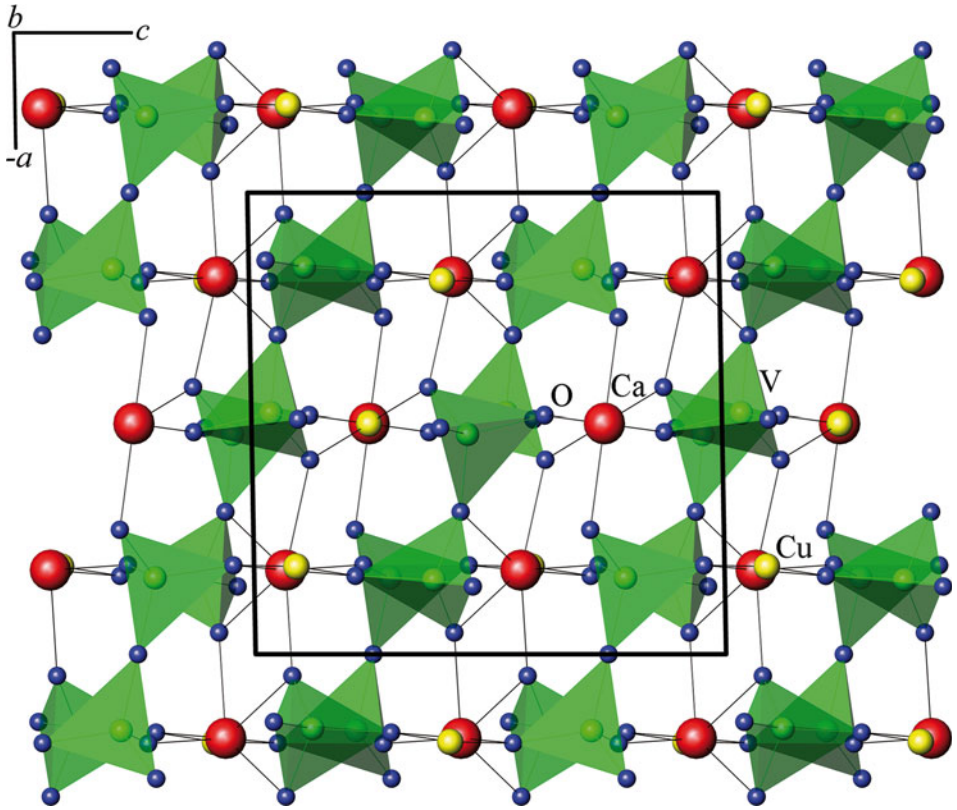

Figure 6. (Color online) Orientation of groups $V_2O_7^{4-}$ in $CaCuV_2O_7$ (Vogt and Muller-Buschbaum, 1991b).

https://doi.org/10.1017/S0885715618000441 Published online by Cambridge University Press

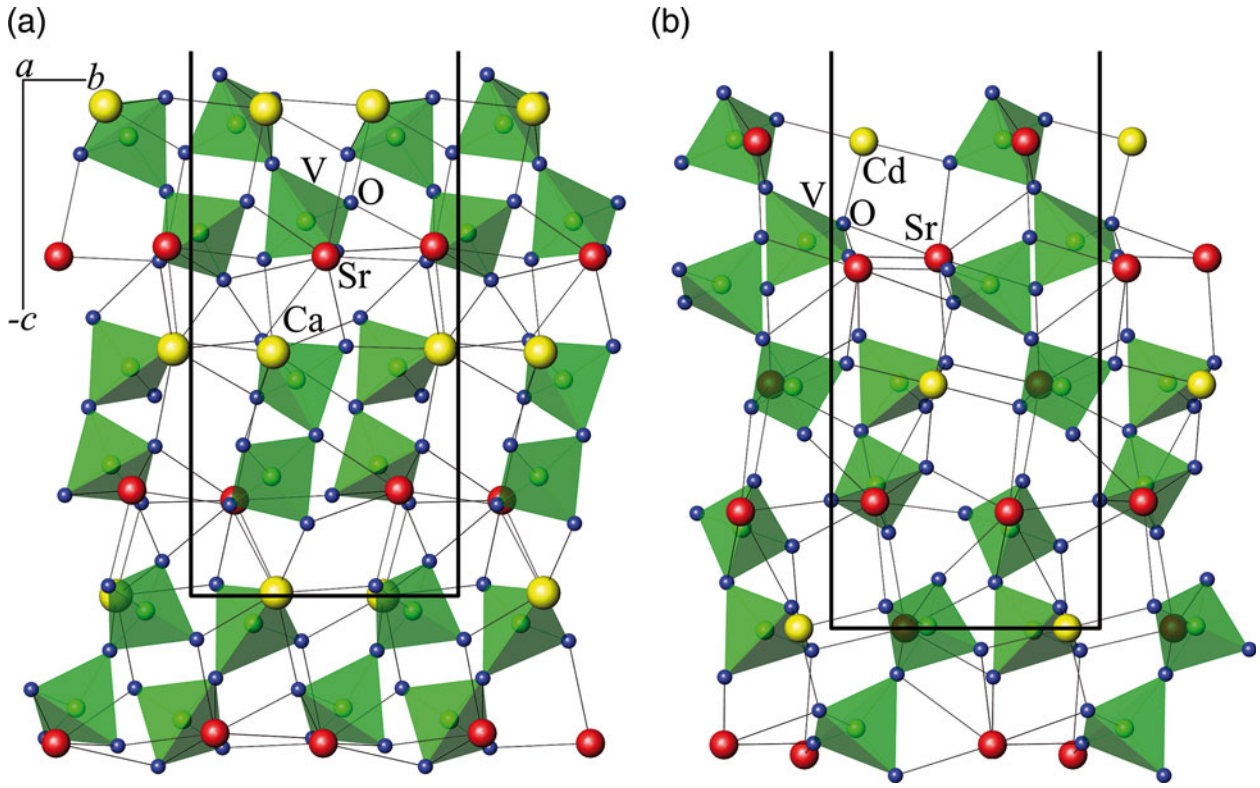

Figure 7. (Color online) The projection of fragments of the structure of (a) $Sr_3Ca(V_2O_7)_2$ and (b) $Sr_3Cd(V_2O_7)_2$ along the ***a***-axis.

$(V_2O_7)_2$ and $Sr_3Cd(V_2O_7)_2$, and also $Sr_3Ca(V_2O_7)_2$ with space group $P4_1$ (Figure 7) are identified.

Proceeding from the arrangement (configuration) of oxygen polyhedrons in vanadium crystal lattices of double vanadates $MM^I{}_2V_2O_7$, $M_3M^I(V_2O_7)_2$, $MM^I{}_2(V_4O_{14})$, $M_3M^I(V_3O_{10})(VO_4)$, they can be considered as derivatives of pyrovanadate *M*2V2O7 of the type of potassium dichromate ($M_2V_2O_7$, *M* = Ba, Sr, Co, Ni, Pb) or calcium pyrovanadate $Ca_2V_2O_7$. The variety of crystal structures inside these two families is because of the arrangement of two types of bivalent cations and rotation of vanadium–oxygen polyhedrons. For pyrovanadates $M_2V_2O_7$ having a thortveitite structure, the formation of broad primary solid solutions in their binary systems is more typical. Both in the pyrovanadates $M_2V_2O_7$ and in the double vanadates of divalent metals, structural transformations associated with the evolution of "soft" metal–oxygen polyhedra can take place when the temperature or the composition are changed (Krasnenko *et al.*, 2017; Rotermel and Krasnenko 2017).

IV. CONCLUSIONS

Two new double vanadates $Ca_2Zn_2(V_4O_{14})$ (I) and $Pb_2Cd_2(V_3O_{10})(VO_4)$ (II) have been synthesized, and their crystal structures have been described. The double vanadates of divalent metals known to date can be classified in six different groups according to the proximity of their crystal structures to the structure of vanadium–oxygen anions. The crystal lattices of double vanadates of divalent metals can be regarded as being derived from two types of pyrovanadates *M*2V2O7 with the structure of potassium dichromate or calcium pyrovanadate.

SUPPLEMENTARY MATERIAL

The supplementary material for this article can be found at https://doi.org/10.1017/S0885715618000441.

ACKNOWLEDGEMENTS

The studies are carried out in accordance with the plans of the Institute of Solid State Chemistry of the Ural Branch of the Russian Academy of Sciences (НИОКТР АААА-А16-116122810216-3, А16-116122810218-7).

Altomare, A., Cuocci, C., Giacovazzo, C., Moliterni, A., Rizzi, R., Corriero, N., and Falcicchio, A. (**2013**). "EXPO 2013: a kit of tools for phasing crystal structures from powder data," J. Appl. Crystallogr. **46**, 1231–1235.

Babaryk, A. A., Odynets, I. V., Khainakov, S., Garcia-Granda, S., and Slobodyanik, N. S. (**2015**). "Polianionic identity of $Ca_2Zn_2(V_3O_{10})(VO_4)$ photocatalyst manifested by X-ray powder diffraction and periodic boundary density functional theory calculations," CrystEngComm **17**(40), 7772–7777.

Basiev, T. T., Voronko, Yu. K., Maslov, V. A., Sobol, A. A., and Shukshin, V. E. (**2011**). "Lead pyrovanadate single crystal as a new SRS material," Quantum Electron., **41**(2), 125–127.

Bhatia, S. N., Moharatra, N., Nirmala, R., and Malik, S. (**2010**). "The effect of spin dilution on magnetism of the linear chain system β-$Cu_{2-x}Zn_xV_2O_7$," Pramana J. Phys. **74**(5), 833–843.

Cid-García, A., Lozada-Morales, R., López-Calzada, G., Zayas Ma, E., Angel, O. Z., Carmona-Rodriguez, J., Rodriguez-Melgarejo, F., Rubio-Rosas, E., Jiménez-Sandoval, S., and Tomás, S. A. (**2012**). "Room temperature photoluminescence in crystalline/amorphous Er-doped $Cd_2V_2O_7$," J. Lumin. **132**(6), 1511–15114.

Cowin, P. I., Lan, R., Petit, C. T. G., Christophe, T. G., Zhang, L., and Tao, S. (**2011**). "Conductivity and stability of cobalt pyrovanadates," J. Alloys Compd. **509**(10), 4117–4121.

Dalal, M., Taxak, V. B., Lohra, S., Sangvan, D., and Khatkar, S. P. (**2015**). "Photoluminescence and structural properties of Eu^{3+} doped $SrZnV_2O_7$ nanocrystals," J. Lumin. **161**, 63–70.

Felsche, J. (**1970**). "Polymorphism and crystal data of the rare-earth disilicates of type $R.E._2 Si_2O_7$," J. Less Common Met. **21**(1), 1–14.

Felsche, J. (**1972**). "A new silicate structure containing linear (Si_3O_{10}) groups," Naturwissenschaften **59**(1), 35–36.

Krasnenko, T. I., Slobodin, B. V., Zabara, O. A., Fotiev, A. A., and Kiseleva, N. V. (**1990**). "Phase relations in the system V_2O_5-$Na_4V_2O_7$-$Ca_2V_2O_7$-$Cd_2V_2O_7$," Russ. J. Inorg. Chem. **35**, 1553–1556.

Krasnenko, T. I., Rotermel, M. V., and Samigullina, R. F. (**2017**). "Stabilizing the associated non-autonomous phase upon thermal expansion of $Zn_2V_2O_7$," Russ. J. Inorg. Chem. **62**, 412–417.

Larson, A. C. and Von Dreele, R. B. (**2004**). *General Structure Analysis System (*GSAS*)*. (Report LAUR 86-748) (Los Alamos National Laboratory, Los Alamos, New Mexico).

Murashova, E. V., Velikodnyi, Yu. A., and Trunov, V. K. (**1989**). "Crystal structures of double pyrovanadates $BaMV_2O_7$ (M = Ca, Cd, Zn)," Russ. J. Inorg. Chem. **34**, 1388–1392.

Murashova, E. V., Velikodnyi, Yu. A., and Trunov, V. K. (**1991**). "Crystal structures of double pseudo pyrovanadates PbM'V_2O_7 (M' = Mg, Zn)," Kristallografiya **36**, 617–621.

Murashova, E. V., Velikodnyi, Yu. A., Yluchin, A. V., and Zhuravlev, V. D. (**1993a**). "Crystal structures of $Sr_{1.58}Ca_{0.42}V_2O_7$ $Sr_{1.5}Cd_2V_2O_7$ and the singularities of their isomorphism," Russ. J. Inorg. Chem. **38**, 428–431.

Murashova, E. V., Velikodnyi, Yu. A., and Zhuravlev, V. D. (**1993b**). "Crystal structures of double pyrovanadates $CaMgV_2O_7$ и $CaCoV_2O_7$," Russ. J. Inorg. Chem. **38**, 1453–1454.

Murashova, E. V., Velikodnyi, Yu. A., and Zhuravlev, V. D. (**1994**). "Crystalline structure of $Ca_{1.22}Cd_{0.78}V_2O_7$ solid solution," Russ. J. Inorg. Chem. **39**, 738–739.

ICDD. (**2016**). *PDF-2 (Database)*, edited by Dr. Soorya Kabekkodu (International Centre for Diffraction Data, Newtown Square, PA, USA).

Rietveld, H. M. (**1969**). A profile refinement method for nuclear and magnetic structures. J. Appl. Crystallogr. **2**, 65–71.

Rotermel, M. V. and Krasnenko, T. I. (**2017**). "The mechanism of thermal expansion of structural modifications of zinc pirvanadate", Kristallografiya **62**, 549–556.

Sanchez-Andujar, M., Yáñez-Vilar, S., Mira, J., Biskup, N., Rivas, J., Castro-García, S., and Señarís-Rodríguez, M. A. (**2011**). "Role of the magnetic ordering on the dielectric response of $M_2V_2O_7$ (M = Co and Cu) divanadates," J. Appl. Phys. **109**, 054106, https://doi.org/10.1063/1.3556448.

Sivakumar, T., Chang, H. Y., and Halasyamani, P. S. (**2007**). "Synthesis, structure, and characterization of a new two-dimensional lead (II) vanadate, $Ba_3PbV_4O_{14}$," Solid State Sci. **9**(5), 370–375.

Shannon, R. D. (**1976**). "Revised effective ionic radii and systematic studies of interatomic distances in halides and chalcogenides," Acta Crystallogr. Sect. A Cryst. Phys. Diffr. Theor. Gen. Crystallogr. **32**, 751–767.

Takahashi, M., Hagiwara, M., and Fujihara, S. (**2016**). "Liquid-phase synthesis of $Ba_2V_2O_7$ phosphor powders and films using immiscible biphasic organic–aqueous systems," Inorg. Chem. **55**(16), 7879–7885.

Toby, B. H. (**2001**). "EXPGUI, a graphical user interface for GSAS," J. Appl. Crystallogr. **34**, 210–213.

Velikodnyi, Yu. A. and Murashova, E. V. (**1992**). "The crystal structure of SrCuV2O7 and the structural series SrMV2O7 (M = Cu,Zn,Mg,Sr)," Kristallografiya **37**, 818–820.

Velikodnyi, Yu. A., Trunov, V. K., Kudin, O. V., and Zhuravlev, V. D. (**1985**). "Crystal structure of dual pyrovanadate of strontium-magnesium," Kristallografiya **30**, 663–667.

Velikodnyi, Yu. A., Murashova, E. V., and Trunov, V. K. (**1989**). "Crystal structure of double pyrovanadate $SrZnV_2O_7$," Kristallografiya **34**, 607–610.

Vogt, R. and Muller-Buschbaum, Hk. (**1991a**). "Bacuv$_2$o$_7$: Das letzte Glied der Reihe $MCuV_2O_7$ ($M = Mg^{2+}$, Ca^{2+}, Sr^{2+}, Ba^{2+})," J. Less Common Met. **171**(2), L35–L39.

Vogt, R. and Muller-Buschbaum, Hk. (**1991b**). "Der Übergang von planaren zu tetraedrischen CuO_4-Baugruppen in $CaCuV_2O_7$," Z. Anorg. Allg. Chem. **594**(1), 119–126.

Werner, P. E., Eriksson, L., and Westdahl, M. (**1985**). "TREOR, a semi-exhaustive trial-and-error powder indexing program for all symmetries," J. Appl. Crystallogr., **18**(5), 367–370.

Zhuravlev, V. D. and Velikodnyi, Yu. A. (**1990**). "System SrO–CaO–V_2O_5," Russ. J. Inorg. Chem. **35**, 264–266.

Zhuravlev, V. D. and Velikodnyi, Yu. A. (**1997**). "Isomorphic substitutions in systems $Pb_2V_2O_7$–$M_2V_2O_7$, где M = Ba, Sr, Ca, Cd," Russ. J. Inorg. Chem. **42**, 1387–1389.

Zhuravlev, V. D., Velikodnyi, Yu. A., and Surat, L. L. (**1993**). "X-ray study of systems $Mn_2V_2O_7$–$Mn_2V_2O_7$, где M = Ba, Sr, Ca, Zn, Cu, Ni," Russ. J. Inorg. Chem. **38**, 1221–1224.

Zhuravlev, V. D., Surat, L. L., and Velikodnyi, Yu. A. (**1994**). "Phase diagrams of the systems $Mn(VO_3)_2$-$M(VO_3)_2$ и $Mn_2V_2O_7$-$M_2V_2O_7$ (M – Sr, Ba)," Neorg. Mater., **30**, 1574–1575.

Zhuravlev, V. D., Fotiev, A. A., Zhukov, V. P., and Kristallov, L. V. (**1982**). "Research systems $Mg_2V_2O_7$–$Sr_2V_2O_7$, $Zn_2V_2O_7$–$M_2V_2O_7$ (M = Mg, Ca, Sr)," Russ. J. Inorg. Chem, **27**, 1018–1021.